Dye-Sensitized Nanostructured p-Type Nickel Oxide Film as a Photocathode for a Solar Cell

Jianjun He, Henrik Lindström, Anders Hagfeldt, and Sten-Eric Lindquist*

Department of Physical Chemistry, Uppsala University, Box 532 S-751 21 Uppsala, Sweden

Received: May 24, 1999; In Final Form: August 12, 1999

Nanostructured NiO film was prepared by depositing nickel hydroxide slurry on conducting glass and sintering at 500 °C to a thickness of about 1 μm. The photocurrent−voltage (IV) characteristics of the plain nanostructured NiO electrode recorded potentiostatically in a standard three-electrode setup upon UV illumination demonstrate p-type behavior, while the IV characteristics of a dye-sensitized nanostructured NiO electrode coated with erythrosin B show cathodic photocurrent under visible light illumination. The highest incident photon-to-current conversion efficiencies of tetrakis(4-carboxyphenyl)porphyrin (TPPC) and erythrosin B-coated NiO films were 0.24% and 3.44%, respectively. In sandwich solar cells with a platinized conducting glass as counter electrode exposed to light from a sun simulator (light intensity: 68 mW/cm^2), a short-circuit cathodic photocurrent density (I_{SC}) of 0.079 mA/cm^2 and an open-circuit voltage (V_{OC}) of 98.5 mV for TPPC-coated NiO electrode were achieved. Similarly, $I_{SC} = 0.232$ mA/cm^2 and $V_{OC} = 82.8$ mV were registered when the NiO electrode was coated with erythrosin B. The cathodic photocurrent is explained by hole injection from dye molecule to the valence band of the p-NiO electrode.

The overall solar-to-electric conversion efficiency of nanostructured n-TiO_2 film coated with cis-di(thiocyanato)-*N*,*N*-bis-(2, 2′-bipyridyl-4, 4′-dicarboxylic acid)-ruthenium(II) has reached 10%.[1,2] Recent studies have been focused on the mechanisms and kinetics of charge injection into the TiO_2 and charge transport in the nanostructured electrode.[3−8] The possibilities of using other nanostructured n-type semiconductors, e.g., ZnO,[9] other sensitizing dyes,[10] and solid-state electrolytes,[11] in dye-sensitized solar cells (DSCs) have been investigated. However, to our knowledge, no reports have appeared concerning dye-sensitized nanostructured p-type large band gap semiconducting electrodes. In the case of dye-sensitized nanostructured n-type semiconducting electrodes, visible-light absorption by the sensitizing dye is followed by electron transfer from the excited state of dye to the conduction band of the semiconductor. The dye is regenerated by electron transfer from the reduced species, usually I^-, in the electrolyte to the oxidized dye, the injected electron in the conduction band diffuses to the back contact, and the reduced species in the electrolyte is recovered at the counter electrode. In our present study, we investigate TPPC and erythrosin B-coated nanostructured p-type NiO films as working electrodes in DSCs. NiO is known as a large band gap (3.6−4.0 eV) semiconductor with a tendency to be of p-type as prepared.[12−14] The HOMO levels of the chosen dyes are below the energy level of the top of the valence band, E_{VB}, while the LUMO levels are above the energy level of the redox system (I^-/I_3^-) and far below the energy level of the bottom of the conduction band, E_{CB}. The optical excitation of the adsorbed dye is followed by (a) electron transfer from the excited dye to the oxidized species (I_3^-) in the electrolyte, and (b) electron transfer from valence band of p-type NiO to the HOMO level of the dye (See Figure 1). The hole in the valence band diffuses to the back contact. The oxidized species in the electrolyte are regenerated at the counter electrode. From the present study we are not able to determine in which order (a) and (b) above take place.

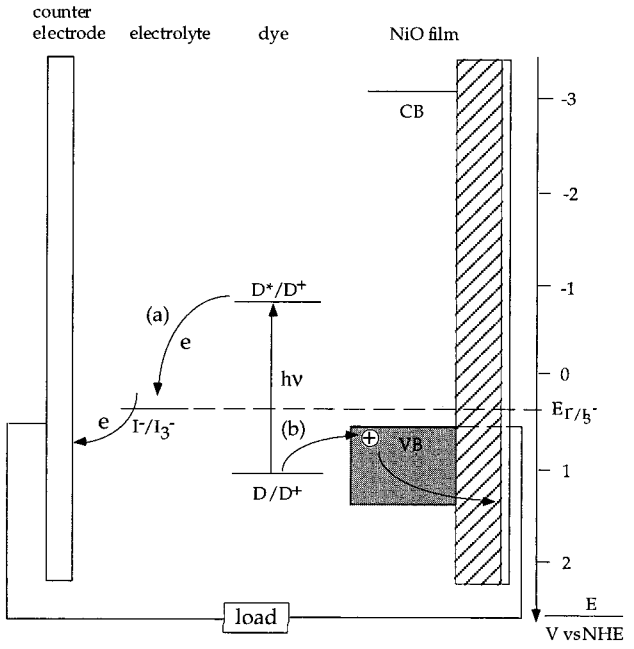

Figure 1. Schematic diagram illustrating the energetics of dye-sensitized nanostructured p-NiO solar cell for which we take TPPC as an example.

Porous nickel oxide films were prepared by depositing nickel hydroxide slurry produced from hydrolysis of nickel acetate[15] on the conducting glass (Libbey Owens Ford, 8 ohm/square), followed by sintering in air at 500 °C for 1 h. The thickness of the film was about 1 μm. Thicker layers cracked under the sintering. Scanning electron microscopy (SEM) of the film indicated that the film was highly porous and the particle size

* Corresponding author.

10.1021/jp991681r CCC: $18.00
Published on Web 09/30/1999

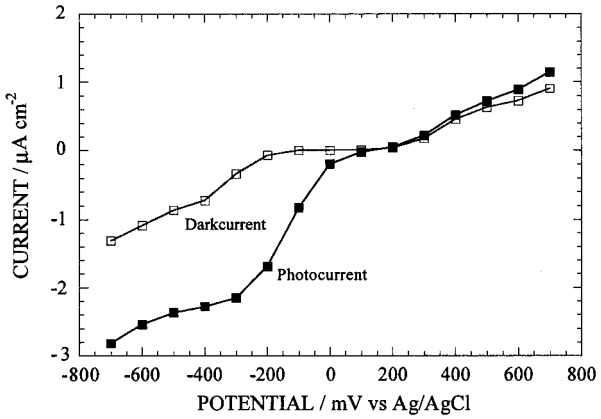

Figure 2. Current vs potential curves for nanostructured NiO electrode in 0.1 N $LiClO_4$ aqueous solution with a buffer of 0.01 M HPO_4^{2-} and 0.01 M $H_2PO_4^-$ (pH 6.8) in a standard three-electrode setup. The light source is a xenon 450 W lamp. The beam passed through an 80 mm filter of water in a quartz vessel and then through a quartz window before it reached the front side of the NiO film working electrode. The distance between the lamp and the working electrode is about 50 cm. The solution was deaerated with nitrogen for over 20 min prior to the measurements and bubbled with nitrogen and stirred throughout the measurements. At each potential applied, the dark current and photocurrent had reached plateaus.

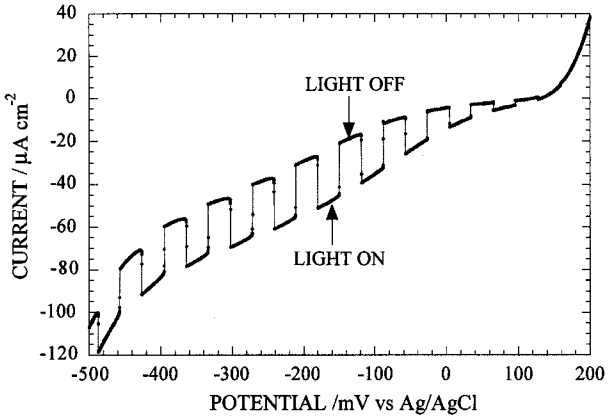

Figure 3. Current vs potential curves for nanostructured NiO film coated with erythrosin B in 0.1 M LiI/0.01 M I_2 propylene carbonate using intermittent light from a sun simulator (light intensity: 85 mW/cm^2) swept from 200 mV to −500 mV vs Ag/AgCl. Scan rate was 0.1 mV/s. Interval time of light illumination was 5 min. The light reached the dye-coated NiO electrode from substrate side. The solution was deaerated with nitrogen for over 20 min prior to the measurements and bubbled with nitrogen and stirred throughout the measurements.

was 10−20 nm. Dye-coating of the NiO film was carried out by soaking the film electrode in an ethanol solution of TPPC or erythrosin B while the electrode was still hot, ca. 80 °C. The current−voltage (IV) characteristics of the plain nanostructured NiO electrode recorded potentiostatically in a standard three-electrode setup are shown in Figure 2. The curves in dark and under UV illumination (450 W xenon lamp full light) demonstrate p-type behavior of the NiO electrode with an onset of photocurrent at approximately +100 mV vs Ag/AgCl reference electrode but only a few microampere photocathodic current.

The IV characteristics of the same nanostructured NiO electrode coated with erythrosin B illuminated intermittently using light from a sun simulator (light intensity: 85 mW/cm^2) are shown in Figure 3. The cathodic photocurrent is now much higher, approximately 100 μA/cm^2 in the plateau region, and the onset is increased to approximately +150 mV vs Ag/AgCl reference. The p-type behavior is again unambiguously demonstrated.

Figure 4 shows the absorption spectra of TPPC and erythrosin B in ethanol solutions and on the NiO films and the photocurrent action spectra obtained for NiO films coated with TPPC and erythrosin B in sandwich-type cells. One can see that the absorption spectra of TPPC and erythrosin B on NiO films shift to red region, and the spectrum of erythrosin B on NiO is broader than that in the ethanol solution. Such extensive change in the absorption spectra indicates a relatively strong adsorption interaction between the dye and the semiconductor surface.[16] It is also seen that these shifts are further enhanced comparing the action spectra with the dyes/NiO absorption spectra. This further enhancement could be attributed to an adsorption interaction being stronger in the excited state than in the ground state.[17] The photocurrent action spectra resemble the absorption spectra pretty well. It is of value to note that the photocurrent is cathodic, being opposite to that in Grätzel-type DSC. The highest IPCE value for TPPC-coated NiO electrode is 0.24% at the wavelength of 540 nm, in which only Q-bands are taken into account, and for erythrosin B-coated NiO electrode is 3.44% at the wavelength of 560 nm.

Figure 5 shows the photocurrent-photovoltage characteristics of the sandwich-type cells illuminated by a sun-simulated light (light intensity: 68mW/cm^2). The dye-coated NiO electrode was squeezed together with a platinized conducting glass using a spring. The electrolyte, 0.5 M LiI/0.05 M I_2 in ethylene carbonate/propylene carbonate (1/1 by weight), was filled into the interelectrode space by capillary forces. For a TPPC-coated NiO cell (Figure 5a), the short-circuit photocurrent (I_{SC}) was 0.079 mA/cm^2, open-circuit photovoltage (V_{OC}) 98.5 mV, fill factor (FF) 28.5%, and overall conversion efficiency (η) 0.0033%, and for the erythrosin B−NiO cell (Figure 5b), the corresponding values were I_{SC} = 0.232 mA/cm^2, V_{OC} = 82.8 mV, FF = 27.0%, and η = 0.0076%. The overall conversion efficiency is very low because of the small photocurrent and photovoltage. The effects of incident light intensity on the short-circuit photocurrent and open-circuit photovoltage for the erythrosin B-coated NiO electrode are shown in the inset to Figure 5b. With increasing the light intensity, the open-circuit photovoltage increases and reaches a plateau. This means that the Fermi level in the NiO electrode is lowered with increasing light intensity, approaching the upper edge of the valence band, E_{VB}, at high light intensities. The short-circuit photocurrent is increasing and leveling off with light intensity, reaching a limiting value at high intensities. This indicates losses of the holes in the VB because of reactions with reduced species in the electrolyte and/or excited dye molecules.

The energetics of dye-sensitized nanostructured p-NiO solar cells in which we take the energetics of TPPC as examples are shown in Figure 1. The flatband potential of the NiO semiconductor is about 0.95 V vs NHE in 1.0 N H_2SO_4.[18] This gives approximately a position of valence band of NiO around 0.54 V vs NHE at pH 7.0. The HOMO levels of TPPC[19,20] and erythrosin B[21] are 1.01 V and 1.19 V vs NHE, respectively, well below the energy level of the top of the valence band, E_{VB}, while the LUMO levels are at −0.90V and −1.11 V vs NHE, respectively, that is, above the energy level of the redox system (I^-/I_3^-, 0.44 V vs NHE[22]) and well below the energy level of the bottom of the conduction band (E_{CB} = −3.06 V vs NHE). When exciting the sensitizing dye with visible light, the excited state of the dye can from its LUMO level transfer an electron to the oxidized species in the electrolyte. It is thermodynamically impossible for the excited state of the dye to inject electron to the conduction band of the semiconductor. The dye is regenerated by hole injection from the oxidized dye

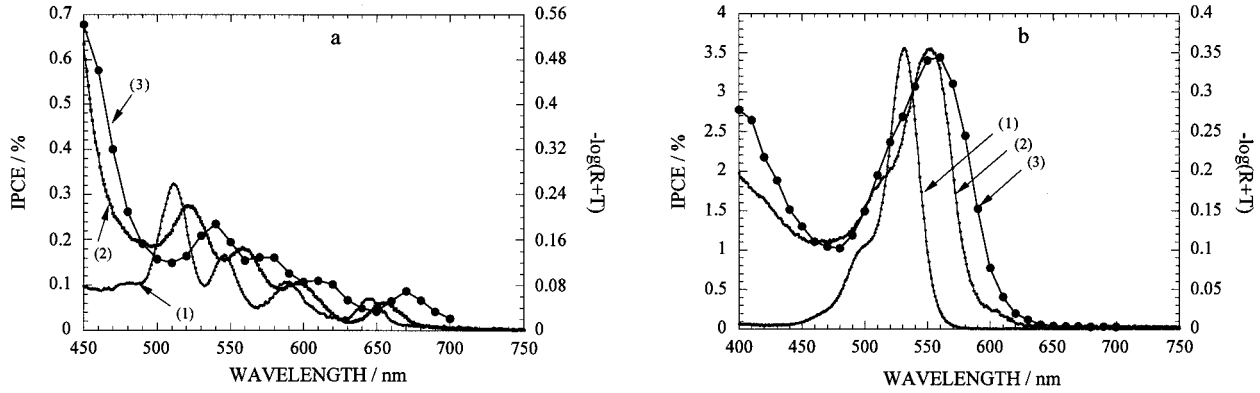

Figure 4. Absorption spectra ($-\log(R+T)$) of TPPC (a) and erythrosin B (b) in ethanol solutions (curves 1, [TPPC] = 1.5×10^{-5} M; [erythrosin B] = 3.4×10^{-6} M.) and on the nanostructured films measured in an integrating sphere (curves 2). Action spectra (curves 3) of nanostructured NiO films coated with TPPC (a) and erythrosin B (b) in sandwich-type measurements. The working electrode of dye-coated film on conducting glass was squeezed together with a platinum foil using a spring and illuminated from substrate side. The electrolyte, 0.5 M LiI/0.05 M I_2 in ethylene carbonate/propylene carbonate (1/1 by weight), was attracted into the cavities of the dye-coated NiO electrode by capillary forces. The cell was operated in the short-circuit mode.

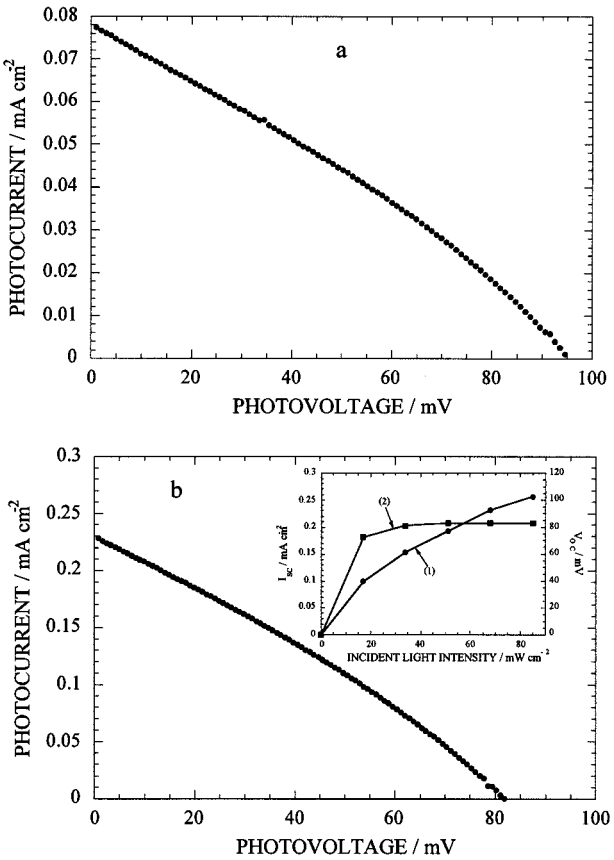

Figure 5. Photocurrent−photovoltage characteristics of nanostructured NiO electrodes coated with TPPC (a) and erythrosin B (b). The electrolyte was 0.5 M LiI/0.05 M I_2 in ethylene carbonate/propylene carbonate (1/1 by weight). The cells were exposed to light from a sun simulator (light intensity: 68 mW/cm^2). The surface area of each cell was about 0.25 cm^2. The inset to Figure 5b shows the effects of incident light intensity on the short-circuit photocurrent (curve 1) and open-circuit photovoltage (curve 2) for the erythrosin B-coated NiO electrode.

to the valence band of the semiconductor. The injected hole diffuses to the back contact and the oxidized species in the electrolyte is recovered on the counter electrode. This results in a cathodic photocurrent which is confirmed by our experiments (see Figures 3 and 4). It is expected that the Fermi level of the semiconductor would be lowered and reach at open-circuit conditions the upper edge position of the valence band, E_{VB}, at high light intensities. The photogenerated potential difference would then be the difference between the potential of level of the valence band, E_{VB}, in the photocathode and the potential of the redox couple, E_{redox}, that is, the maximum possible photovoltage would be $V_{OC} = |E_{VB} - E_{redox}|$. As the energy level of I^-/I_3^- is 0.44 V vs NHE, thus the expected photovoltage is around 0.1 V, which is confirmed by our experiments.

Although the cathodic photocurrent, photovoltage, and overall conversion efficiency all are very small because of the rather positive redox potential of the redox couple and/or the relatively negative energy level of the valence band of the semiconductor and the thinness of the nanostructured NiO film, the principle of the dye-sensitized nanostructured p-type semiconducting photocathode in a solar cell is important. We are currently trying different redox couples which have relatively negative redox potential and/or other large band gap p-type semiconductors which have more positive valence band energy level than that of p-NiO, to enlarge the difference between the potential of level of the valence band (E_{VB}) in the photocathode and the potential of the redox couple (E_{redox}). Complete results of the optimization will be presented elsewhere. Furthermore, it is expected that the combination of a photocathode and a photoanode in a well-matched couple in tandem cell will increase significantly the photovoltage as well as the overall conversion efficiency.

Acknowledgment. The Swedish National Energy Administration, MISTRA, and Swedish Research Council for Engineering Sciences are acknowledged. We also thank Dr. Licheng Sun at Department of Organic Chemistry, Royal Institute of Technology for his helpful discussions and kind supply of tetrakis(4-carboxyphenyl)porphyrin (TPPC).

References and Notes

(1) O'Regan, B.; Grätzel, M. *Nature* **1991**, *353*, 737−740.

(2) Nazeeruddin, M. K.; Kay, A.; Rodicio, I.; Humphry-Baker, R.; Müller, E.; Liska, P.; Vlachopoulos, N.; Grätzel, M. *J. Am. Chem. Soc.* **1993**, *115*, 6382−6390.

(3) Tachibana, Y.; Moser, J. E.; Grätzel, M.; Klug, D. R.; Durrant, J. R. *J. Phys. Chem.* **1996**, *100*, 20056−20062.

(4) Hannappel, T.; Burfeindt, B.; Storck, W.; Willig, F. *J. Phys. Chem. B* **1997**, *101*, 6799−6802.

(5) Ellingson, R. J.; Asbury, J. B.; Ferrere, S.; Ghosh, H. N.; Sprague, J. R.; Lian, T.; Nozik, A. J. *J. Phys. Chem.* B **1998**, *102*, 6455−6458.

(6) Södergren, S.; Hagfeldt, A.; Olsson, J.; Lindquist, S.-E. *J. Phys. Chem.* **1994**, *98*, 5552−5556.

(7) Solbrand, A.; Lindström, H.; Rensmo, H.; Hagfeldt, A.; Lindquist S.-E.; Södergren, S. *J. Phys. Chem.* B **1997**, *101*, 2514−2518.

(8) Lindström, H.; Rensmo, H.; Södergren, S.; Solbrand A.; Lindquist, S.-E. *J. Phys. Chem.* **1996**, *100*, 3084−3088.
(9) Rensmo, H.; Keis, K.; Lindström, H.; Södergren, S.; Solbrand, A.; Hagfeldt, A.; Lindquist, S.-E.; Wang L. N.; Muhammed, M. *J. Phys. Chem*. B **1997**, *101*, 2598−2601.
(10) Kay, A.; Grätzel, M. *J. Phys. Chem*. **1993**, *97*, 6272−6277.
(11) Bach, U.; Lupo, D.; Comte, P.; Moser, J. E.; Weissörtel, F.; Salbeck, J.; Spreitzer H.; Grätzel, M. *Nature* **1998**, *395*, 583−585.
(12) Adler, D.; Feinleib, J. *Phys. Rev*. B **1970**, *2*, 3112−3134.
(13) Sato, H.; Minami, T.; Takata, S.; Yamada, T. *Thin Solid Films* **1993**, *236*, 27−31.
(14) Miller, E. L.; Rocheleau, R. E. *J. Electrochem. Soc*. **1997**, *144*, 1995−2003.
(15) Liu, K.-C.; Anderson, M. A. *J. Electrochem. Soc*. **1996**, *143*, 124−130.
(16) Kamat, P. V. *Chem. Rev.* **1993**, *93*, 267−300.
(17) Gerischer, H.; Willig, F. *Top. Curr. Chem*. **1976**, *61*, 31−84.
(18) Tench, D. M.; Yeager, E. *J. Electrochem. Soc.* **1973**, *120*, 164−171.
(19) Vergeldt, F. J.; Koehorst, R. B. M.; Schaafsma, T. J.; Lambry, J.-C.; Martin, J.-L.; Johnson, D. G.; Wasielewski, M. R. *Chem. Phys. Lett*. **1991**, *182*, 107−113.
(20) Kalyanasundaram, K.; Neumann-Spallart, M. *J. Phys. Chem*. **1982**, *86*, 5163−5169.
(21) Kamat, P. V.; Fox, M. A. *Chem. Phys. Lett*. **1983**, *102*, 379−384.
(22) Hagfeldt, A.; Grätzel, M. *Chem. Rev*. **1995**, *95*, 49−68.